Solvent−Solute Interactions Probed by Picosecond Transient Raman Spectroscopy: Vibrational Relaxation and Conformational Dynamics in S_1 *trans*-4,4′-Diphenylstilbene

James D. Leonard, Jr.[†] and Terry L. Gustafson*

Department of Chemistry, The Ohio State University, 100 West 18th Avenue, Columbus, Ohio 43210-1185

Received: July 19, 2000; In Final Form: January 8, 2001

We present the S_1 picosecond transient Raman spectra of *trans*-4,4′-diphenylstilbene (DPS) obtained at excitation wavelengths of 287 and 310 nm and probe wavelengths of 630 and 660 nm. We compare spectra at different pump and probe wavelengths in order to evaluate the role of conformational dynamics and vibrational relaxation in S_1 DPS. In this study, we find that dioxane and methylene chloride accept excess vibrational energy from the photoexcited solute in a different manner. We attribute this variation either to a difference in the local solvent structure or to the difference in the density of states between methylene chloride and dioxane. We also find that the relative intensities of certain bands demonstrate a dependence upon the pump and probe wavelengths. From these data, we have established that the change in relative intensity with delay is a marker for the dynamical shift in the S_1 potential energy surface. The dependence of this dynamical change on excitation wavelength demonstrates that we are examining a "nonstationary" state that evolves on a 10−50 ps time scale.

Introduction

Relaxation processes in the excited state, including vibrational and conformational relaxation, provide insight into the fundamental interactions that occur between a solute and its solvent environment.[1−38] Experimentally, the approach for determining the effect of solvent on excited state relaxation processes is to generate the excited state photolytically and monitor the rate at which some property of the excited state changes while varying the solvent properties systematically. The reaction rates are then compared to bulk properties of the solvent, since the solvent is viewed as noninteracting from the perspective of statistical mechanics (i.e., the solvent molecules simply act as a heat bath that may be considered as a continuous viscous medium at liquid-phase densities). The primary tools used to study these interactions have been time-resolved fluorescence and absorption spectroscopies.

We and others have shown that picosecond transient Raman spectroscopy provides a valuable tool for the examination of solute−solvent interactions.[2,4−7,10,13−18,22,24−28,39−57] An advantage of time-resolved Raman spectroscopy is that it provides mode-specific information about the probe molecule so that solvent-induced structural effects may be observed directly. Dynamical effects are observed in transient Raman spectra as changes in bandwidth, peak position, and relative intensity with time delay. The transient spectra provide sensitive vibrational markers for solvation dynamics.

Several picosecond transient Raman studies have been performed by our group and others on *trans*-stilbene (tS) in various solvents to gain insight into the effect of solvent and excess vibrational energy on the S_1 tS molecule.[10,13−15,17,18,42−46,49,53,56−58] Derivatives of tS have also been examined in order to gain further insight into solute−solvent interactions and to gather more evidence for relaxation theories that have been proposed to describe the behavior of tS. Morris and Gustafson have reported S_1 transient Raman results for 1,4-diphenyl-1,3-butadiene (DPB) in several solvents.[4,5] They observe peak position and bandwidth changes for the olefin stretch of the 1^1B_u mode of DPB.[4] They attribute the changes to vibrational relaxation of the DPB molecule. Transient Raman spectra of paraphenylenes have been studied by Hamaguchi and co-workers in order to examine the effect of chain length on the delocalization of π electron excitation.[3,16,59] Their results for *para*-terphenyl indicate that a very fast structural change occurs in this molecule within 5 ps of photoexcitation. The authors suggest that this change is due to a torsional motion that involves the C−C bonds that link the phenyl rings.[16] Butler et al. have reported the picosecond transient Raman spectra of *trans*-4,4′-diphenylstilbene (DPS) in dioxane and methylene chloride.[40] They observe only small shifts in the peak positions and bandwidths of the transient Raman bands with time delay in both solvents at the excess vibrational energies used in their study. However, the relative intensities of S_1 Raman bands that have been assigned to the biphenyl portions of the molecule show significant changes with delay and are affected by variation of the solvent environment.[40] Butler et al. interpret the changes in relative intensity for these bands to indicate that the molecule is assuming a more planar conformation following photoexcitation. The rate of this change is affected by the solvent dielectric constant which, the authors suggest, helps to stabilize the increased electron density on the phenyl rings.[40] Leonard and Gustafson have shown that the conformation of DPS in aromatic solvents is affected by substituents on the solvent phenyl rings, while vibrational relaxation is essentially identical in the solvents studied.[2]

In this work, we present picosecond transient Raman spectra of DPS obtained at two excitation wavelengths and two probe wavelengths. We compare spectra at these wavelengths for S_1 DPS in dioxane and methylene chloride solutions. As we have

* Corresponding author. Phone: 614-292-1832. Fax: 614-292-1685. E-mail: gustafson.5@osu.edu.

[†] Present address: Chemicals Technology, Eastman Chemical Co., P.O. Box 511, Kingsport, TN 37662-5231.

10.1021/jp002586h CCC: $20.00
Published on Web 02/21/2001

reported previously for DPS, we observe solvent-dependent, mode-specific dynamic behavior for several bands. We compare spectra at different pump wavelengths in order to examine the role of excess vibrational energy in conformational and vibrational relaxation. We observe that the magnitude of the peak shift for S_1 DPS in methylene chloride is greater than the magnitude of the peak shift with delay for S_1 DPS in dioxane at comparable excess vibrational energies (relative to the 0−0 transition). This indicates that methylene chloride accepts excess vibrational energy from the solute in a different manner than does dioxane. We find that the relative intensities of the Raman bands are dependent upon both pump and probe wavelengths. We also observe that the dynamics of the change in relative intensity with delay are different when examined with different probe wavelengths indicating that the S_1 potential energy surface is a "nonstationary" state that evolves on a picosecond time scale.

Instrumentation

The megahertz laser system that we use to obtain picosecond transient Raman spectra has been described previously.[39,40,58] Briefly, the second harmonic of a continuous wave mode-locked Nd:YAG laser (Coherent, Inc., Model Antares 76S) is used to pump two independently tunable, cavity-dumped, synchronously pumped dye lasers (Coherent, Inc., Models 702-2 and 702-3). The excitation media are R6G (Exciton Corp.) and DCM (Exciton Corp.) with saturable absorber solutions of DQOCI (Exciton Corp.) and DTDCI (Exciton Corp.), respectively. The output from the R6G dye laser is amplified at megahertz repetition rates in a six pass amplifier that is pumped by a cavity dumped argon ion laser (Coherent, Inc., Model Innova 200 with a Model 7208 cavity dumper).[39] The amplified output is then frequency doubled by an angle-tuned KDP crystal (Spectra-Physics, Model 390) thus providing 20−40 nJ/pulse with a temporal width of 3 ps in the region of ca. 280−315 nm. The visible probe pulse is delayed via an optical delay line (Compumotor F-L5A-P54) before being combined collinearly with the UV pump beam and focused on the sample. The polarization of the pump and probe beams are set to magic angle (54.7°) in order to avoid contributions to the transient Raman spectra resulting from rotational reorientation effects.[60] We use a spinning sample cell to minimize photoproduct buildup in the cell. The pump and probe beams impinge on the sample at a 45° angle, and the backscattered Raman signal is dispersed through a single stage monochromator (ISA THR640) using a 600 g/mm grating. A CCD multichannel analyzer (Photometrics CC200 System with Thomson-CSF 576 × 384 chip) is used to detect the signal.

To minimize the formation of a long-lived photoproduct of DPS, we found it necessary to change the samples during routine pauses in the experiment. Continuous exposure time for one sample was approximately 0.5 min. Data acquisition was controlled by a PC running software written in ASYST (Asyst Software Technologies).[61] The wavenumber shift was calibrated using the Raman spectra of acetone and benzene. Data collection times were 10 and 20 min at each delay for the dioxane solutions and methylene chloride solutions, respectively. The spectra were analyzed using software written in ASYST[61] and using Peakfit (Jandel Scientific). Raman bands were fit to Lorenztian profiles.

DPS was purchased from Lancaster Chemical (scintillation grade, 2039-68-1) and was used without further purification. For the Raman experiments, we prepared saturated solutions of DPS in methylene chloride (Mallinckrodt, spectrophotometric grade, 75-09-2) and dioxane (E. M. Science, scintillation grade, 123-91-1). The concentration of the solutions were 1.5 and 0.5 mM for methylene chloride and dioxane, respectively, as determined by UV−vis absorption spectroscopy.

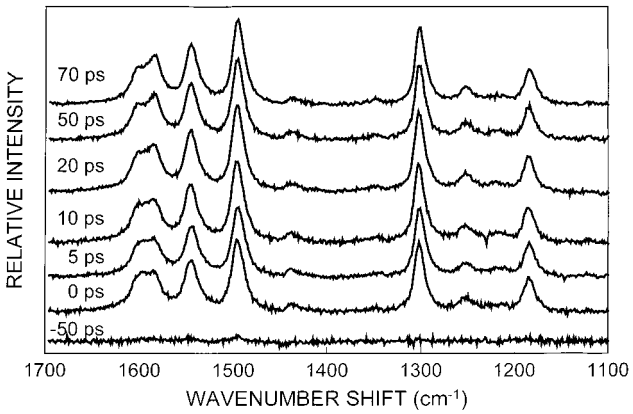

Figure 1. S_1 transient Raman spectra of *trans*-4,4′-diphenylstilbene in dioxane at various delays from −50 to 70 ps after photoexcitation with 310 nm radiation: probe, 660 nm; repetition rate, 1 MHz. Each delay represents the unsmoothed spectrum obtained by 10 min of total observation time.

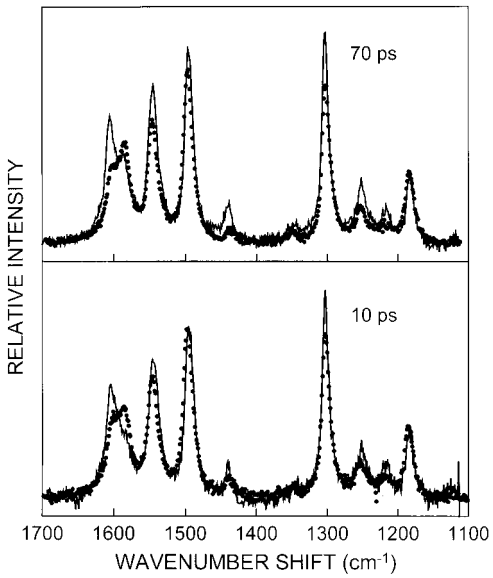

Figure 2. Comparison of S_1 transient Raman spectra of DPS in dioxane (solid line) and methylene chloride (dashed line) at time delays of 10 ps (bottom) and 70 ps (top) following photoexcitation: pump, 310 nm; probe, 660 nm.

Results

We have obtained picosecond transient Raman spectra of DPS in dioxane and methylene chloride over the range from 1100 to 1700 cm^{-1} at various delays. We have obtained spectra at two excitation wavelengths, 310 and 287 nm, corresponding to ∼5300 and ∼7900 cm^{-1} of excess vibrational energy, respectively, above the 0−0 transition for DPS (∼27 000 cm^{-1}). Spectra at each pump wavelength were obtained at probe wavelengths of 630 and 660 nm. In Figure 1, we present the spectra of S_1 DPS in dioxane at delays of −50, 0, 5, 10, 20, 50, and 70 ps. The excitation wavelength for these data is 310 nm with a probe wavelength of 660 nm. All of the spectra presented in this paper have been normalized to the 1185 cm^{-1} band as described previously.[40] In Figure 2, we compare spectra of S_1 DPS in dioxane and methylene chloride at time delays of 10

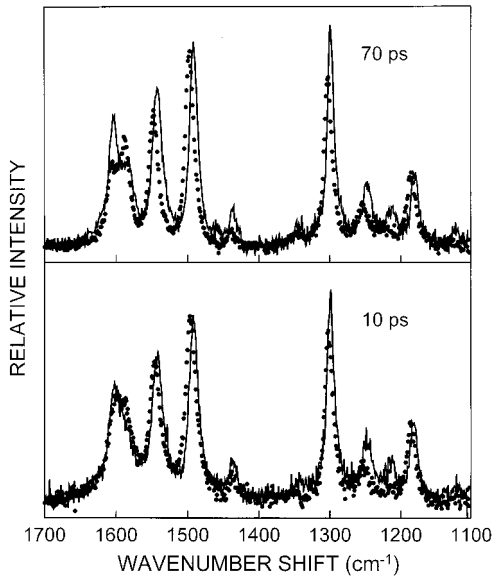

Figure 3. Comparison of S_1 Raman spectra of DPS in dioxane (solid line) and methylene chloride (dashed line) at time delays of 10 ps (bottom) and 70 ps (top) following photoexcitation: pump, 287 nm; probe, 660 nm.

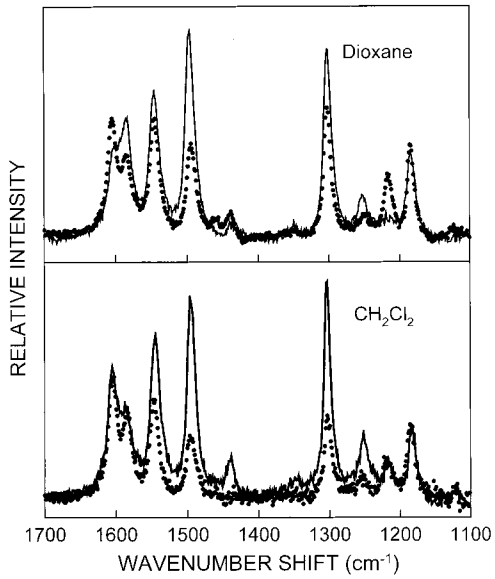

Figure 4. Comparison of the probe wavelength dependence of S_1 Raman spectra of DPS in dioxane (top) and methylene chloride (bottom). Excitation wavelength: 310 nm. Probe wavelengths: 630 nm (dashed line) and 660 nm (solid line). Both sets of spectra have been normalized to the Raman band at 1185 cm^{-1}.

and 70 ps with an excitation wavelength of 310 nm and a probe wavelength of 660 nm. In these spectra, it is clear that there are significant differences between solvents in the relative intensities of several bands. To show the effect of changing the amount of excess vibrational energy in the DPS molecule, we present Figure 3 which shows spectra taken with an excitation wavelength of 287 nm and a probe wavelength of 660 nm. From these data, we observe that Raman bands associated with the "biphenyl-like" portions of the molecule demonstrate the largest differences in relative intensity between solvents.[40] In Figure 4, we present a comparison of the S_1 Raman spectra of DPS in dioxane and methylene chloride obtained with 310 nm excitation and probed at 630 and 660 nm. We note that the relative intensities of several bands are enhanced in the 660 nm spectra relative to the spectra acquired with a 630 nm probe.

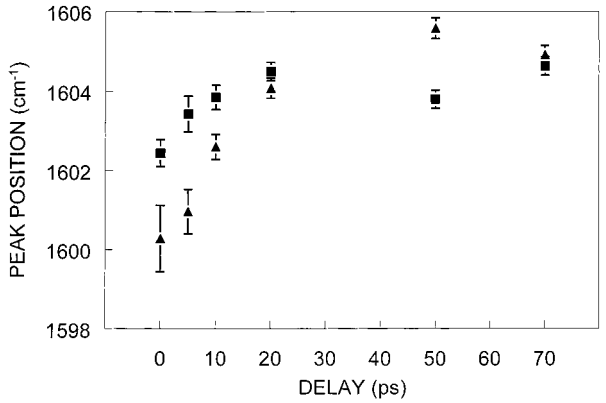

Figure 5. Peak position of the olefin C═C stretching vibration of S_1 DPS in dioxane vs delay for two pump wavelengths: 310 nm (■) and 287 nm (▲). Probe: 630 nm.

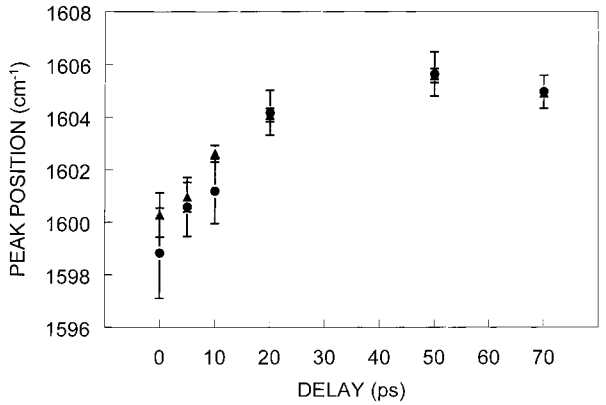

Figure 6. Peak position of the olefin C═C stretching vibration of S_1 DPS in dioxane vs delay for two probe wavelengths: 630 nm (▲) and 660 nm (●). Pump: 287 nm.

Discussion

A. Vibrational Relaxation.

Several research groups have shown that the peak shift with delay of excited-state Raman bands is a marker for vibrational relaxation in S_1 tS.[2,4,5,14,16,18,42−44,47,49,55,56,58,62,63] We observe a similar phenomenon in DPS. In Figure 5, we plot the peak position of the olefin band versus delay for DPS in dioxane at excitation wavelengths of 287 and 310 nm. Error bars represent $\pm 2\sigma$ limits in the fits. The rate of peak position change for both excitation wavelengths appears similar; however, the position of the olefin band with 287 nm excitation starts out at a lower frequency. We attribute the dynamics observed at different excitation wavelengths to vibrational relaxation of the solute molecule. Similar results have been reported for tS in alkane solvents.[4,5,14,42,44,47,49,56,58] We note that other bands demonstrate shifts with delay and upon changing excitation frequency. We find, however, that only the 1605, 1585, and 1546 cm^{-1} bands exhibit bandwidth changes with delay within our experimental error (the data are not shown). The band at 1605 cm^{-1} has been assigned to the olefin mode of the DPS molecule while the 1585 cm^{-1} band has been attributed to phenyl C═C stretching motions.[40] The 1546 cm^{-1} band has been assigned to a "biphenyl-like" motion of the molecule involving the inter-ring stretch.[40] In Figure 6, we plot the peak position change versus delay for the 1605 cm^{-1} band of DPS in dioxane with an excitation wavelength of 287 nm and probe wavelengths of 630 and 660 nm. We observe that there is no difference in the vibrational relaxation dynamics between the two probe wavelengths. The dependence of the peak position shift on pump

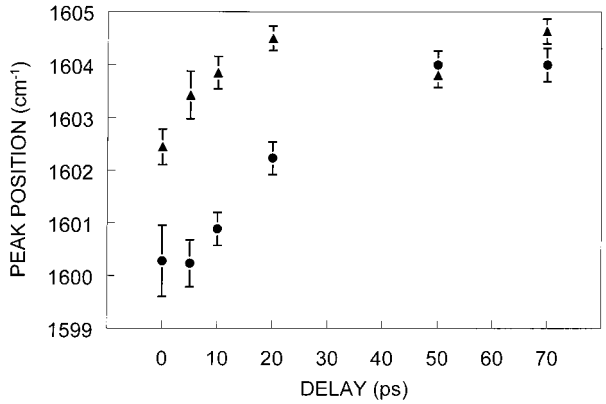

Figure 7. Comparison of the peak position shift of the olefin C═C band of S_1 DPS in methylene chloride (●) and dioxane (▲) with 310 nm excitation and 630 nm probe.

wavelength and the independence of the peak position shift on probe wavelength is strong evidence that the peak position change is a marker for vibrational relaxation dynamics. We note that we attempted to obtain the time-resolved anti-Stokes Raman spectra of DPS, an experiment that has been effective at elucidating vibrational relaxation. The fluorescence from the solute precluded us from obtaining any useful information from these experiments.

To examine the solvent dependence of the vibrational relaxation of DPS, we have obtained S_1 Raman spectra of DPS in dioxane and methylene chloride. For the 1605 cm^{-1} band of DPS in methylene chloride at excitation wavelengths of 287 and 310 nm with a probe wavelength of 630 nm, the dynamics of the peak position shift are nearly identical for the two pump wavelengths (the data are not shown). We present a comparison between dioxane and methylene chloride for this same band at an excitation wavelength of 310 nm and a probe wavelength of 630 nm in Figure 7. It is clear that the magnitude of the peak shift is greater for DPS in methylene chloride than for DPS in dioxane at this pump wavelength. When we use a pump wavelength of 287 nm, the magnitude of peak shift for this same band is the same for S_1 DPS in both dioxane and methylene chloride (the data are not shown). In separate experiments, we have determined that the 0−0 transition of DPS does not shift appreciably between these two solvents.

This variation of peak position change with solvent indicates that methylene chloride and dioxane accept excess vibrational energy from the solute differently. Jean and co-workers suggested that the thermal diffusivity of a solvent may be important in the thermal cooling of a vibrationally excited solute molecule.[43] They indicate that the relative insensitivity of vibrational relaxation rates in S_1 tS to different solvents environments may be due to the fact that diffusion of energy out of the first solvent shell into the bulk solvent may be the rate-controlling step. Iwata and Hamaguchi independently quantified the way that vibrational relaxation depends on the thermal properties of the solvent.[13−15] In their model, the thermal diffusivity of the solvent controls the rate of cooling between the solvent molecules nearest the solute and the bulk solvent. For the data presented in Figure 7, we fit the change in peak position to a single exponential. The lifetimes for the vibrational relaxation in methylene chloride and dioxane are 36 and 6.3 ps, respectively. The thermal diffusivities of methylene chloride and dioxane are 8.81×10^{-8} and 8.91×10^{-8} m^2/s, respectively.[2] The result for dioxane is consistent with values obtained for vibrational cooling in tS in solvents with similar thermal diffusivities by Iwata and Hamaguchi.[14] On the basis of our results, the rate of vibrational relaxation is more than five times slower in methylene chloride than in dioxane. In view of the similar thermal properties of methylene chloride and dioxane, our results indicate that other factors must also contribute to the vibrational relaxation process. We suggest that there are two possible explanations for the differences between methylene chloride and dioxane. The first possibility is that the structure of the solvent in the first solvent shell is significantly different between the two solvents. The solvent structure would affect the rate of energy transfer between the solute and the first solvent shell. Several studies provide supporting evidence for this idea. Morris and Gustafson have interpreted the anomalous behavior of the band attributed to phenyl stretching motions in 1,4-diphenyl-1,3-butadiene in pentane, where there is an absence of dynamics in peak position relative to other linear alkanes, to a difference in the solvent structure.[5] Rice and Baronazski have observed an anomalously long lifetime for *cis*-stilbene (cS) in cyclohexane that they attribute to the specific way in which the solvent molecules interact with the cS molecule.[64] In addition, Jiang and Blanchard have presented results for perylene in various alkane solvents that indicate the presence of short range order in the solvent cage surrounding the solute molecule.[65] The second possibility is the difference in the solvent bath modes that are available to accept the excess vibrational energy from the solute. One would predict that variations in the density of states in the low-frequency range would affect the coupling between the low-frequency modes in DPS and the solvent. The greater density of states in dioxane would provide for more efficient coupling with the low-frequency S_1 vibrational states of DPS relative to the solvent bath modes in methylene chloride. Additional studies of DPS and other solutes in a range of solvents will provide insight into the relative contributions of solvent structure and solvent density of states in controlling the rate of vibrational relaxation in the excited state.

B. Conformational Dynamics.

Conceptually, the transient resonance Raman phenomenon must be considered as originating from a nonstationary state (i.e., the structure of the S_1 state is evolving with time). An evolving S_1 structure can give rise to dynamical variations in the relative intensities of the Raman bands owing to a change in the Franck−Condon overlap between S_1 and the resonant state, S_n, with time. In a previous paper, we interpreted the changes in relative intensity with delay as an indication that the structure of S_1 DPS evolves to a more planar geometry following photoexcitation.[40] A test of this interpretation would be that the dynamics of the relative intensity change should be probe wavelength dependent since a different region of the Franck−Condon surface will be probed at different probe wavelengths at different delays. In general, we observe this phenomenon. In Figure 8, we present a plot of relative intensity versus delay for the 1493 cm^{-1} band of S_1 DPS in methylene chloride at two different probe wavelengths at an excitation wavelength of 287 nm. The intensities were normalized to that of the 1185 cm^{-1} band as described previously.[40] It is clear from this plot that the dynamics are different depending upon the probe wavelength. For the 630 nm probe, the change in relative intensity is essentially complete 10 ps following photoexcitation. However, the change in relative intensity for the 660 nm probe is not complete until approximately 35 ps. This provides evidence that the S_1 state is evolving with time and that an important method for probing this evolution is through the use of multiple probe wavelengths that are decoupled from the excitation wavelength. We note that only those

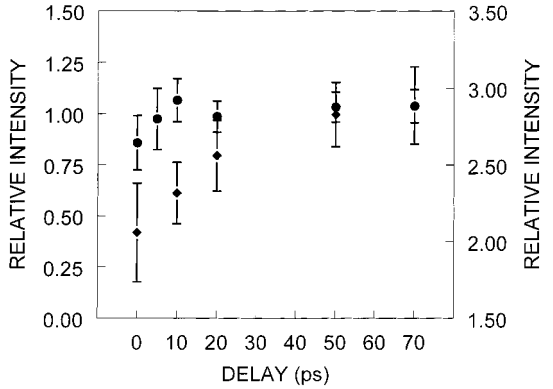

Figure 8. Relative peak intensity of the 1490 cm^{-1} band, scaled to the 1185 cm^{-1} band, as a function of delay for DPS in methylene chloride at probe wavelengths of 630 nm (●) and 660 nm (◆). The uncertainty corresponds to $\pm 2\sigma$ in the fit. Excitation wavelength: 287 nm.

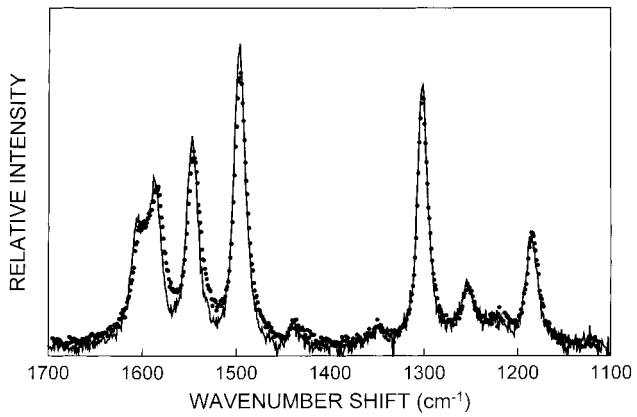

Figure 9. S_1 Raman spectra of DPS in dioxane over the region 1100−1700 cm^{-1} at two pump wavelengths: 310 nm (solid line); 287 nm (dashed line). Time delay: 70 ps. Probe: 660 nm. Repetition rate: 1 MHz for both spectra.

bands containing contributions from the inter-ring stretch exhibit this phenomenon.

We also observe a dependence of the relative intensity on the pump wavelength at certain probe wavelengths. When we compare the S_1 Raman spectra of DPS obtained with two pump wavelengths (287 and 310 nm) and a probe wavelength of 630 nm at 70 ps following photoexcitation, there is not a perceptible difference between the spectra (the data are not shown). However, at a probe wavelength of 660 nm, there are certain bands that tend to exhibit a higher intensity at an excitation wavelength of 287 nm. Figure 9 shows a comparison of the S_1 Raman spectra of DPS obtained at a probe wavelength of 660 nm and excitation wavelengths of 287 and 310 nm. The time delay in this plot is 70 ps. We observe that bands which we attribute to the "biphenyl-like" portions of the molecule show higher relative intensity when pumped with 287 nm excitation as compared to 310 nm excitation. The dynamics of the change in relative intensity for the 1546 cm^{-1} band at a probe wavelength of 630 nm do not change with excitation wavelength (the data are not shown). In Figure 10, we plot the relative intensity versus delay for the same band and excitation wavelengths but at a probe wavelength of 660 nm. There are significant differences between the dynamics of the 287 and 310 nm excitation data. This difference in the observed behavior of certain bands suggests that the excess vibrational energy increases the Franck−Condon overlap for some of the vibrational modes. This also indicates that the population in the "hot"

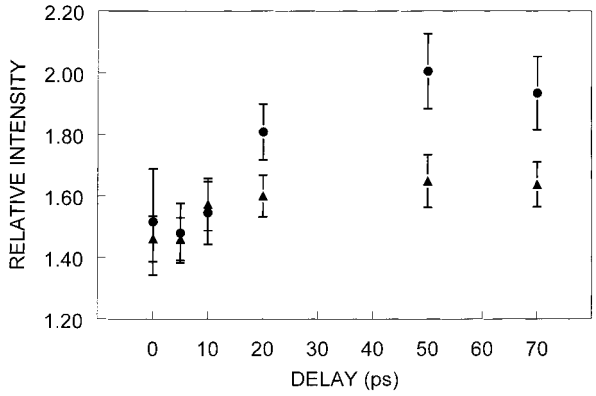

Figure 10. Relative peak intensity of the 1540 cm^{-1} band, scaled to the 1185 cm^{-1} band, as a function of delay for DPS in dioxane at pump wavelengths of 287 nm (●) and 310 nm (▲). The uncertainty corresponds to $\pm 2\sigma$ in the fit. Probe wavelength: 660 nm.

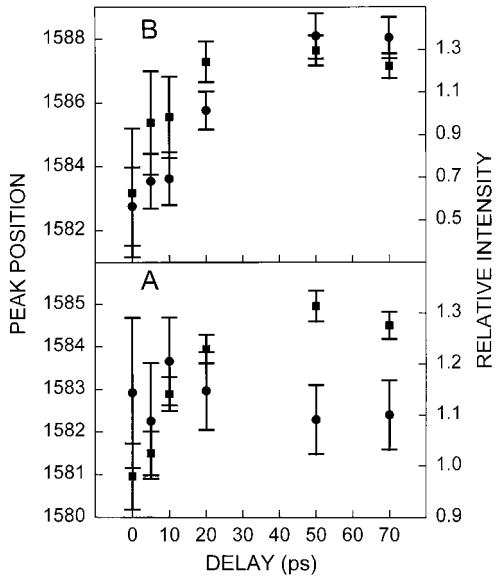

Figure 11. Comparison of the vibrational and conformational relaxation rates for the phenyl C═C stretch of S_1 DPS. Peak position shift (■, left axis) and relative peak intensity (●, right axis) are plotted versus time delay at probe wavelengths of 660 nm (A) and 630 nm (B). Pump wavelength: 287 nm. Repetition rate: 1 MHz.

low-frequency vibrations provide additional Franck−Condon overlap between the S_1 and S_n states for certain modes. This may arise because the modes involved in the conformational relaxation are also those modes that are involved in the vibrational relaxation of the molecule, namely the phenyl−phenyl torsional vibrations. We observe population in these low-frequency modes through the presence of overtone and combination bands in the 1800 cm^{-1} region of the spectrum (the data are not shown).

We can test this hypothesis by comparing the dynamics of the peak position change which is our marker for vibrational relaxation and the dynamics of the relative intensity change which represents our marker for conformational change. Where the relative intensity changes with delay, the dynamics appear to be indistinguishable from the dynamics of peak position change. In Figure 11, we present a comparison of these dynamics for the 1585 cm^{-1} band of S_1 DPS which corresponds to the phenyl C═C stretch. We observe that, for a probe wavelength of 630 nm, the dynamics are not the same for peak position change and relative intensity change with delay (plot A of Figure 11). However, both peak position and relative

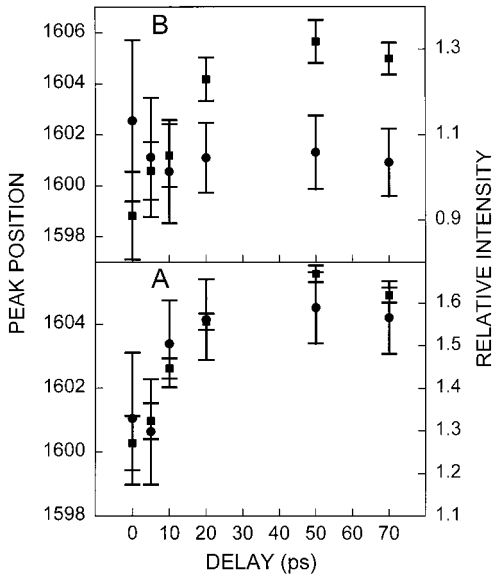

Figure 12. Comparison of the vibrational and conformational relaxation rates for the olefin C═C stretch of S_1 DPS. Peak position shift (■, left axis) and relative peak intensity (●, right axis) are plotted versus time delay at probe wavelengths of 660 nm (A) and 630 nm (B). Pump wavelength: 287 nm. Repetition rate: 1 MHz.

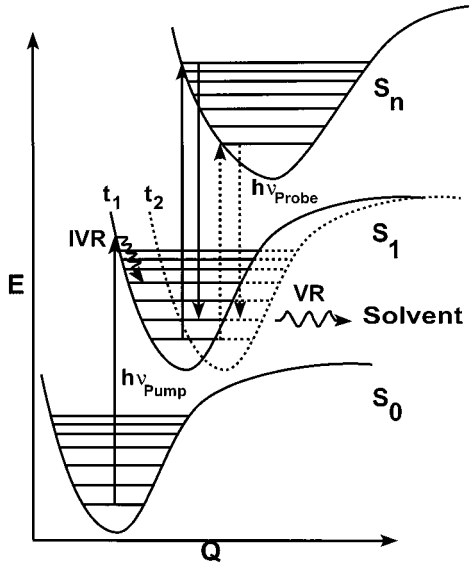

Figure 13. Potential energy diagram for the electronic states of *trans*-4,4′-diphenylstilbene illustrating the time dependence of the vibrational coordinate of the S_1 DPS molecule. Key: *E*, energy; *Q*, vibrational coordinate; IVR, intramolecular vibrational relaxation; t_x, time with t_1 (solid lines) ≠ t_2 (dashed lines); VR, vibrational relaxation via resonance energy exchange with the solvent.

intensity follow the same trend when the sample is examined with a probe of 660 nm (plot B of Figure 11). In this case, the relative intensity change with delay tracks that of the change in peak position. Figure 12 shows similar plots for the 1605 cm^{-1} band that corresponds to the olefin C═C stretching frequency. In this set of plots we observe that the relative intensity changes with delay at a probe wavelength of 630 nm (plot A of Figure 12), but the relative intensity does not change with delay with a 660 nm probe (plot B of Figure 12). The picture that emerges upon consideration of these plots is that there is a connection between the dynamics of the vibrational relaxation and the conformational dynamics that occur on the S_1 surface.

A schematic representation of these phenomena is presented in Figure 13. The times t_1 and t_2 in Figure 13 represent some arbitrary times following photoexcitation before the S_1 population decays to the ground state. The vertical arrows from the S_1 state represent different probe wavelengths. Shortly after photoexcitation into the S_1 electronic state (<1 ps), the excess vibrational energy that is deposited initially in the Franck−Condon modes of the molecule is redistributed. Iwata and Hamaguchi have shown that the intramolecular vibrational relaxation (IVR) process results in a "hot" solvent shell around the solute on this time scale.[14,15] We suggest that this model works well for our interpretation of DPS in dioxane but is not consistent with our results for DPS in methylene chloride, where the rate of energy transfer from the solute to the first solvent shell may be limiting. Following this fast IVR, there are two slower (10−50 ps) relaxation processes: (1) The "hot" solvent molecules immediately surrounding the solute will cool by transferring energy to the bulk solvent molecules,[14,15] or as we suggest for DPS in methylene chloride, the solute itself cools and transfers energy to the bulk solvent (VR). (2) The solute can change its conformation along certain nuclear coordinates in order to relax to the optimum equilibrium geometry in the excited state. We note that the conformational coordinate, *Q*, may include solvent rearrangement in addition to an internal molecular coordinate. From this illustration, we observe that, as the S_1 potential energy surfaces evolves with time, the Franck−Condon overlap with the S_n resonant state will change for certain vibrational modes thus providing a consistent explanation of our observations of the probe wavelength dependence of the relative intensities dynamics for certain Raman bands in the S_1 DPS molecule. We would predict that dynamical changes would also appear in the transient absorption spectra of DPS if our interpretation is correct. We have recently verified that there are dynamical changes of the peak positions in the femtosecond transient absorption spectra of DPS in the region where we have obtained transient Raman spectra for this work.[66] Similar effects have also been observed in the transient absorption spectra of quarterphenyl by Matousek et al.[9]

Conclusions

In the present study we have obtained S_1 picosecond transient Raman spectra of *trans*-4,4′-diphenylstilbene at two excitation and two probe wavelengths. We have compared spectra of DPS in methylene chloride and dioxane solutions. We observe that the dependence upon excitation energy is different for DPS in methylene chloride relative to DPS in dioxane. We attribute this variation either to a difference in the local solvent structure or to the difference in the density of states between methylene chloride and dioxane. We find that the relative intensities of certain bands are dependent upon both pump and probe wavelength. We have demonstrated that the dynamics of the change in relative intensity with delay are different when examined with different probe wavelengths which indicates that the S_1 potential energy surface can be modeled as a "nonstationary" state that evolves on a picosecond time scale. We can summarize the observables in transient Raman spectra as follows: changes in the peak position and bandwidth in transient Raman spectra are markers for vibrational relaxation of a solute molecule, while relative intensity changes with delay are an indication of the conformational dynamics of the probe molecule.

Acknowledgment. We acknowledge Coherent, Inc., for the loan of portions of the equipment used in these experiments.

References and Notes

(1) Tan, X.; Gustafson, T. L. *J. Phys. Chem. A* **2000**, *104*, 4469−4474.

(2) Leonard, J. D., Jr.; Gustafson, T. L. *J. Raman Spectrosc.* **2000**, *31*, 353−358.

(3) Hamaguchi, H.; Gustafson, T. L. *Annu. Rev. Phys. Chem.* **1994**, *45*, 593−622.

(4) Morris, D. L.; Gustafson, T. L. *J. Phys. Chem.* **1994**, *98*, 6725−6730.

(5) Morris, D. L.; Gustafson, T. L. *Appl. Phys. B* **1994**, *59*, 389−395.

(6) Kwok, W. M.; Ma, C.; Phillips, D.; Matousek, P.; Parker, A. W.; Towrie, M. *J. Phys. Chem. A* **2000**, *104*, 4188−4197.

(7) Kwok, W. M.; Ma, C.; Matousek, P.; Parker, A. W.; Phillips, D.; Toner, W. T.; Towrie, M. *Chem. Phys. Lett.* **2000**, *322*, 395−400.

(8) Scholes, G. D.; Fournier, T.; Parker, A. W.; Phillips, D. *J. Chem. Phys.* **1999**, *111*, 5999−6010.

(9) Matousek, P.; Parker, A. W.; Towrie, M.; Toner, W. T. *J. Chem. Phys.* **1997**, *107*, 9807−9817.

(10) Matousek, P.; Parker, A. W.; Toner, W. T.; Towrie, M.; Defaria, D. L. A.; Hester, R. E.; Moore, J. N. *Chem. Phys. Lett.* **1995**, *237*, 373−379.

(11) Parker, A. W.; Bisby, R. H. *J. Chem. Soc. Faraday. Trans.* **1993**, *89*, 2873−2878.

(12) Iwata, K.; Hamaguchi, H. *Chem. Lett.* **2000**, 456−457.

(13) Iwata, K.; Hamaguchi, H. *J. Raman Spectrosc.* **1998**, *29*, 915−918.

(14) Iwata, K.; Hamaguchi, H. *J. Phys. Chem. A* **1997**, *101*, 632−637.

(15) Iwata, K.; Hamaguchi, H. *J. Mol. Liq.* **1995**, *65-6*, 417−420.

(16) Iwata, K.; Hamaguchi, H. *J. Raman Spectrosc.* **1994**, *25*, 615−621.

(17) Hamaguchi, H.; Iwata, K. *Chem. Phys. Lett.* **1993**, *208*, 465−470.

(18) Iwata, K.; Hamaguchi, H. *Chem. Phys. Lett.* **1992**, *196*, 462−468.

(19) Iwaki, L. K.; Deak, J. C.; Rhea, S. T.; Dlott, D. D. *Chem. Phys. Lett.* **1999**, *303*, 176−182.

(20) Deak, J. C.; Iwaki, L. K.; Dlott, D. D. *Chem. Phys. Lett.* **1998**, *293*, 405−411.

(21) Hong, X. Y.; Chen, S.; Dlott, D. D. *J. Phys. Chem.* **1995**, *99*, 9102−9109.

(22) Waele, V. D.; Buntinx, G.; Poizat, O.; Flament, J. P. *J. Raman Spectrosc.* **2000**, *31*, 275−281.

(23) Buntinx, G.; Naskrecki, R. *J. Phys. Chem.* **1996**, *100*, 19380−19388.

(24) Bremard, C.; Buntinx, G.; De Waele, V.; Didierjean, C.; Gener, I.; Poizat, O. *J. Mol. Struct.* **1999**, *480−481*, 69−81.

(25) Didierjean, C.; De Waele, V.; Buntinx, G.; Poizat, O. *Chem. Phys.* **1998**, *237*, 169−181.

(26) Didierjean, C.; Buntinx, G.; Poizat, O. *J. Phys. Chem. A* **1998**, *102*, 7938−7944.

(27) De Waele, V.; Buntinx, G.; Poizat, O.; Flament, J. P.; Kassab, E. *J. Chem. Phys.* **1999**, *110*, 6353−6364.

(28) Buntinx, G.; Naskrecki, R.; Didierjean, C.; Poizat, O. *J. Phys. Chem. A* **1997**, *101*, 8768−8777.

(29) Oberle, J.; Abraham, E.; Ivanov, A.; Jonusauskas, G.; Rulliere, C. *J. Phys. Chem.* **1996**, *100*, 10179−10186.

(30) Oberle, J.; Abraham, E.; Ivanov, A.; Jonusauskas, G.; Rulliere, C. *J. Photochem. Photobiol., A* **1997**, *105*, 217−223.

(31) Fleming, G. R. *Chemical Applications of Ultrafast Spectroscopy*, 1st ed.; Oxford University Press: New York, 1986.

(32) Maroncelli, M.; MacInnis, J.; Fleming, G. R. *Science* **1989**, *243*, 1674.

(33) Simon, J. D. *Acc. Chem. Res.* **1988**, *21*, 128.

(34) Barbara, P. F.; Jarzeba, W. *Adv. Photochem.* **1990**, *15*, 1.

(35) Hynes J. T. *Theory of Chemical Reaction Dynamics*; CRC Press: Boca Ratan, FL, 1985; pp 235−260.

(36) Bagchi, B. *Annu. Rev. Phys. Chem.* **1989**, *40*, 115.

(37) Stratt, R. M.; Maroncelli, M. *J. Phys. Chem.* **1996**, *100*, 12981−12996.

(38) Voth, G. A.; Hochstrasser, R. M. *J. Phys. Chem.* **1996**, *100*, 13034−13049.

(39) Weaver, W. L.; Iwata, K.; Gustafson, T. L. *J. Opt. Soc. Am. B* **1993**, *10*, 852−857.

(40) Butler, R. M.; Lynn, M. A.; Gustafson, T. L. *J. Phys. Chem.* **1993**, *97*, 2609−2617.

(41) Iwata, K.; Toleutaev, B.; Hamaguchi, H. *Chem. Lett.* **1993**, 1603−1606.

(42) Hester, R. E.; Matousek, P.; Moore, J. N.; Parker, A. W.; Toner, W. T.; Towrie, M. *Chem. Phys. Lett.* **1993**, *208*, 471−478.

(43) Qian, J.; Schultz, S. L.; Bradburn, G. R.; Jean, J. M. *J. Phys. Chem.* **1993**, *97*, 10638−10644.

(44) Qian, J.; Schultz, S. L.; Bradburn, G. R.; Jean, J. M. *J. Lumin.*. **1994**, *60*, 1727−1730.

(45) Shkurinov, A. P.; Koroteev, N. I.; Jonusauskas, G.; Rulliere, C. *Chem. Phys. Lett.* **1994**, *223*, 573−581.

(46) Qian, J.; Schultz, S. L.; Jean, J. M. *Chem. Phys. Lett.* **1995**, *233*, 9−15.

(47) Nakabayashi, T.; Okamoto, H.; Tasumi, M. *J. Raman Spectrosc.* **1995**, *26*, 841−845.

(48) Poizat, O.; Buntinx, G. *J. Phys. Chem.* **1995**, *99*, 9403−9407.

(49) Towrie, M.; Matousek, P.; Parker, A. W.; Toner, W. T.; Hester, R. E. *Spectrochim. Acta, Part A* **1995**, *51*, 2491−2500.

(50) Yamaguchi, S.; Hamaguchi, H. *Chem. Phys. Lett.* **1994**, *227*, 255−260.

(51) Fujino, T.; Tahara, T. *J. Phys. Chem. A* **2000**, *104*, 4203−4210.

(52) Hogiu, S.; Werncke, W.; Pfeiffer, M.; Elsaesser, T. *Chem. Phys. Lett.* **1999**, *312*, 407−414.

(53) Nakabayashi, T.; Okamoto, H.; Tasumi, M. *J. Phys. Chem. A* **1998**, *102*, 9686−9695.

(54) Jas, G. S.; Wan, C.; Kuczera, K.; Johnson, C. K. *J. Phys. Chem.* **1996**, *100*, 11857−11862.

(55) Nakabayashi, T.; Okamoto, H.; Tasumi, M. *J. Phys. Chem. A* **1997**, *101*, 3494−3500.

(56) Nakabayashi, T.; Okamoto, H.; Tasumi, M. *J. Phys. Chem. A* **1997**, *101*, 7189−7193.

(57) Matousek, P.; Parker, A. W.; Phillips, D.; Scholes, G. D.; Toner, W. T.; Towrie, M. *Chem. Phys. Lett.* **1997**, *278*, 56−62.

(58) Weaver, W. L.; Huston, L. A.; Iwata, K.; Gustafson, T. L. *J. Phys. Chem.* **1992**, *96*, 8956−8961.

(59) Iwata, K.; Yamaguchi, S.; Hamaguchi, H. *Rev. Sci. Instrum.* **1993**, *64*, 2140−2146.

(60) Iwata, K.; Weaver, W. L.; Gustafson, T. L. *Chem. Phys. Lett.* **1993**, *210*, 50−54.

(61) Weaver, W. L. Ph.D. Thesis, The Ohio State University, 1992.

(62) Scholes, G. D.; Matousek, P.; Parker, A. W.; Phillips, D.; Towrie, M. *J. Phys. Chem. A* **1998**, *102*, 1431−1437.

(63) Mizutani, Y.; Kitagawa, T. *Science* **1997**, *278*, 443−446.

(64) Rice, J. K.; Baronavski, A. P. *J. Phys. Chem.* **1992**, *96*, 3359.

(65) Jiang, Y.; Blanchard, G. J. *J. Phys. Chem.* **1994**, *98*, 9411−9416.

(66) Gustafson, T. L.; Lefumeux, C.; Burdzinski, G.; Buntinx, G.; Poizat, O. Unpublished Work.